Anthropogenic influence on recent circulation-driven Antarctic sea ice changes

Journal Article

Author(s):
Haumann, Alexander iD ; Notz, Dirk; Schmidt, Hauke

Anthropogenic influence on recent circulation-driven Antarctic sea ice changes

F. Alexander Haumann[1,2,3], Dirk Notz[1], and Hauke Schmidt[1]

[1]Max Planck Institute for Meteorology, Hamburg, Germany, [2]Environmental Physics, Institute of Biogeochemistry and Pollutant Dynamics, ETH Zürich, Zürich, Switzerland, [3]Center for Climate Systems Modeling, ETH Zürich, Zürich, Switzerland

Abstract Observations reveal an increase of Antarctic sea ice over the past three decades, yet global climate models tend to simulate a sea ice decrease for that period. Here we combine observations with model experiments (MPI-ESM) to investigate causes for this discrepancy and for the observed sea ice increase. Based on observations and atmospheric reanalysis, we show that on multidecadal time scales Antarctic sea ice changes are linked to intensified meridional winds that are caused by a zonally asymmetric lowering of the high-latitude surface pressure. In our simulations, this surface pressure lowering is a response to a combination of anthropogenic stratospheric ozone depletion and greenhouse gas increase. Combining these two lines of argument, we infer a possible anthropogenic influence on the observed sea ice changes. However, similar to other models, MPI-ESM simulates a surface-pressure response that is rather zonally symmetric, which explains why the simulated sea ice response differs from observations.

1. Introduction

Atmospheric circulation changes around Antarctica substantially influence Antarctic sea ice. This relation emerges as an imprint of the Southern Annual Mode (SAM), the dominant mode of circulation variability in the Southern Hemisphere, on interannual sea ice variations [*Stammerjohn et al.*, 2008; *Simpkins et al.*, 2012]. Over the past three decades, the near-surface circulation has significantly intensified, shifting the SAM to more positive phases [*Abram et al.*, 2014]. This is most likely due to anthropogenic stratospheric ozone depletion and greenhouse gas (GHG) increase [*Lee and Feldstein*, 2013; *Abram et al.*, 2014]. However, the response of Antarctic sea ice to this circulation intensification, and thus to the underlying anthropogenic forcing, is not well understood [*Bitz and Polvani*, 2012; *Polvani and Smith*, 2013; *Sigmond and Fyfe*, 2014]. This is owing to the puzzling disagreement between observed and modeled Antarctic sea ice trends and to a lack of process understanding concerning the influence of recent multidecadal atmospheric circulation changes on the sea ice. We here combine observations with model simulations to address both these issues.

Satellite observations show an Antarctic sea ice increase since the late 1970s [*Comiso and Nishio*, 2008], which results from strong opposing regional changes [*Stammerjohn et al.*, 2008]. The sea ice increase in the Ross Sea since the early 1990s is related to enhanced northward ice advection due to stronger southerly winds from Antarctica, whereas advection of warmer air masses from lower latitudes causes a sea ice decrease in that period in the West Antarctic Peninsula (WAP) region [*Haumann*, 2011; *Holland and Kwok*, 2012]. These opposing regional sea ice changes can be explained by a cyclonic circulation anomaly in the region of the Amundsen Sea Low (ASL) [*Turner et al.*, 2009].

These observed circulation and sea ice changes could either be caused by a change in the external forcing or simply be a manifestation of internal variability, which is of comparable magnitude to the observed trend in model simulations [*Polvani and Smith*, 2013; *Zunz et al.*, 2013]. A recent study by *Fan et al.* [2014] supports the latter suggestion by relating multidecadal variations in temperature records to sea ice changes. Such changes in the Antarctic surface climate show connections to the tropical Atlantic [*Li et al.*, 2014; *Simpkins et al.*, 2014] and Pacific [*Ding et al.*, 2011; *Schneider et al.*, 2012] that alter the surface pressure in the ASL region.

In current global models, however, the recent sea ice response seems to be dominated by changes in the external forcing. Otherwise, there would be no reason for coupled global models to consistently
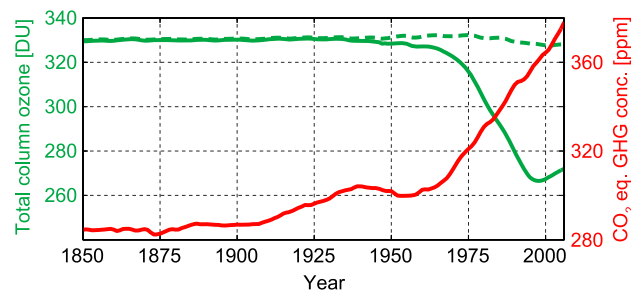
Figure 1. External forcings of model experiments. Red: GHG forcing of Experiments 1 and 2. Green: total column ozone between 63°S and 90°S of Experiments 1 (solid) and 2 (dashed).

simulate an Antarctic sea ice decrease over the observational period [*Mahlstein et al.*, 2013]. This simulated ice loss must hence be a direct response to increasing GHGs, stratospheric ozone depletion, and other external forcings. *Bitz and Polvani* [2012] and *Sigmond and Fyfe* [2014] explain this response by the modeled strengthening and poleward shift of the near-surface westerly winds, which enhances upwelling of warmer water in the Southern Ocean that melts the ice.

These findings contradict the suggestion by *Turner et al.* [2009] that stratospheric ozone depletion could be the cause for the observed sea ice changes.

Here we further explore the possibility of a dominating external driver: Could ozone depletion and/or GHG increase cause the observed sea ice changes if natural variability was not a sufficient explanation? To answer this question, we examine if the observed and the modeled changes in atmospheric circulation and the related sea ice response are consistent with a primarily anthropogenic forcing. Doing so, we also gain insights that explain the disagreement between the modeled and the observed evolution of Antarctic sea ice and tropospheric circulation.

2. Methods, Model, and Data

We compare model simulations to the atmospheric circulation (sea level pressure (SLP), 10 m winds, and geopotential height) from ERA-Interim reanalysis [*Dee et al.*, 2011] and to the observed sea ice concentration [*Meier et al.*, 2013] and drift [*Fowler et al.*, 2013]. The ERA-Interim reanalysis provides the most reliable atmospheric circulation and its changes in the southern high-latitudes among the reanalysis data [*Bracegirdle and Marshall*, 2012]. We use the fully coupled Max Planck Institute for Meteorology Earth System Model (MPI-ESM) in its low-resolution configuration [*Giorgetta et al.*, 2013], which contributed to the Fifth Climate Model Intercomparison Project (CMIP5). The atmospheric component (ECHAM6) [*Stevens et al.*, 2013] is run at a T63 (1.875°) horizontal resolution with 47 vertical hybrid levels reaching up to 0.01 hPa, thus resolving stratospheric changes [*Schmidt et al.*, 2013]. The ocean component (MPIOM) [*Jungclaus et al.*, 2013] has a horizontal resolution of about 1.5° on a bipolar grid with 40 unevenly spaced vertical levels. Sea ice is implemented as a thermodynamic-dynamic model [*Notz et al.*, 2013]. In the Arctic, MPI-ESM realistically simulates the sea ice cover and its response to anthropogenic forcings [*Notz et al.*, 2013]. However, in the Antarctic, it underestimates the mean sea ice extent in all seasons and considerably overestimates its natural variability over the past few decades, as do other CMIP5 models [*Turner et al.*, 2013; *Zunz et al.*, 2013].

We use two sets of simulations that differ in their prescribed stratospheric ozone concentration. One set uses historical GHG emissions and stratospheric ozone depletion (Experiment 1). For this set, we use the three historical simulations carried out with MPI-ESM for CMIP5, covering the period 1850–2005 [*Giorgetta et al.*, 2012a]. The evolution of GHGs and total column ozone [*Cionni et al.*, 2011] in these simulations is shown in Figure 1 (solid lines). A second set of three simulations (Experiment 2) is driven by the same forcings except for stratospheric ozone: We modified the forcing as such that the stratospheric ozone (mixing ratio above 150 ppb) only follows seasonal and interannual variations in the solar irradiance. Anthropogenic changes in stratospheric ozone concentration are hence excluded (Figure 1, green dashed line). Changes in all other forcings such as solar irradiance, tropospheric ozone, and aerosols [*Giorgetta et al.*, 2013] are identical in both experiments. These two experiments allow us to directly study MPI-ESM's response to (1) the combined effect of GHG increase and stratospheric ozone depletion, (2) the effect of GHG increase alone, and (3) the effect of stratospheric ozone depletion alone, where the latter is estimated by examining the difference between the two experiments. In addition, we assess the mean state and internal variability in the model using a 1000 year preindustrial (prior to 1850) control simulation with constant external forcing [*Giorgetta et al.*, 2012b].

We analyze the ensemble mean of three realizations in each respective forcing experiment. Each of these realizations started from different initial conditions taken from the preindustrial control simulation. We use annual means since we are interested in the net response to the forcing. Hence, we neglect possible differences in seasonal variations and trends [*Simpkins et al.*, 2012; *Holland*, 2014]. We calculate linear trends with a least squares regression analysis for the observational period 1979 to 2011 and, to minimize the impact of internal variability, a longer model period from 1960 to 2005 (see the supporting information for details).

3. Results

The annual mean near-surface wind field from the ERA-Interim reanalysis shows that the Antarctic sea ice experiences westerly winds near the ice edge (Figure 2a), whereas most of the coastal and interior sea ice regions experience easterly to southerly winds. The low-pressure belt around Antarctica consists of three distinct climatological SLP minima, with the ASL showing the lowest SLP (Figure 2a). The zonal SLP gradients induced by the asymmetric distribution determine the advection of warmer air masses west of the WAP and the advection of cold continental air over the southwestern Ross and Weddell Seas, influencing the sea ice formation and export [*Haumann*, 2011]. This zonal asymmetry intensifies between 1979 and 2011 (Figure 2c). In particular, the low SLP in the ASL region expands and deepens significantly, leading to increased southerly winds in the western Ross Sea and increased northerly winds in the WAP region. In all other regions the westerlies strengthen. Similar asymmetric structures in the SLP trends have been reported for other reanalysis data sets, but the detailed spatial structure and the magnitude of the trends varies among them [*Bromwich et al.*, 2011].

The meridional wind changes (Figure 2c) go along with a sea ice concentration increase in the Ross Sea and a decrease west of the WAP (Figure 2e). The southerly wind anomaly in the Ross Sea, the expansion of the ASL, and the associated decrease in westerly winds in this region explain the dominating sea ice increase in the western Ross Sea compared to the smaller increase in the eastern Ross Sea. Generally, sea ice drifts at a turning angle of roughly 20° to 40° to the wind direction [*Kottmeier et al.*, 1992]. Consequently, we show that the finding by *Haumann* [2011] and *Holland and Kwok* [2012] that ice drift changes (Figure 2e) are induced by wind changes (Figure 2c), is also evident over the period 1979 to 2011. Potential inconsistencies in the drift trend [*Fowler et al.*, 2013; *Olason and Notz*, 2014] do not affect these results qualitatively (Figure S1 in the supporting information). The increased northward drift in the Ross Sea causes a higher sea ice production at the coast, a higher northward advection, thus an expansion and concentration increase at the ice edge. The decrease in the WAP region is associated with the advection of warmer air masses from lower latitudes [*Haumann*, 2011; *Holland and Kwok*, 2012]. The increase of the total Antarctic sea ice area over the observational period [*Comiso and Nishio*, 2008] is mostly due to a large sea ice area gain in the Ross Sea and a weaker increase in the Weddell Sea, which overcompensate the sea ice decrease in the WAP region.

The preindustrial control simulation also shows three climatological low-pressure areas (Figure 2b) at approximately the same locations as in the reanalysis. However, throughout the entire control simulation neither the observed strength of the ASL nor the observed zonal SLP asymmetry is ever reached. In addition, the modeled ASL is the weakest of the three climatological low-pressure systems. The representation of the ASL is generally poor in current global models [*Hosking et al.*, 2013], which limits the quality of their simulated sea ice. The model additionally overestimates the strength and extent of the coastal easterlies, confining the sea ice at the East Antarctic coast. This rather zonally symmetric circulation is intensified in the historical simulations with all forcings (Experiment 1; 1960–2005; Figure 2d) due to a statistically significant lowering of the SLP with a somewhat stronger response than the changes in the reanalysis. However, the simulated, zonally almost constant, and poleward shifted SLP lowering causes a westerly to northwesterly wind anomaly everywhere.

The model response (Figure 2f) does not reproduce the observed sea ice trends in terms of sign and spatial pattern, which is in line with other models [*Turner et al.*, 2013]. The simulated sea ice changes (1960–2005) are much weaker than the observed ones and amount to an overall decrease. There is a statistically significant ice concentration decrease in the WAP region, in the Weddell Sea, and along the coast of East Antarctica. Also, simulated changes in the ice drift are much weaker than observed and rather zonal. This response of the sea ice agrees with the findings by *Bitz and Polvani* [2012] and *Sigmond and Fyfe* [2014].
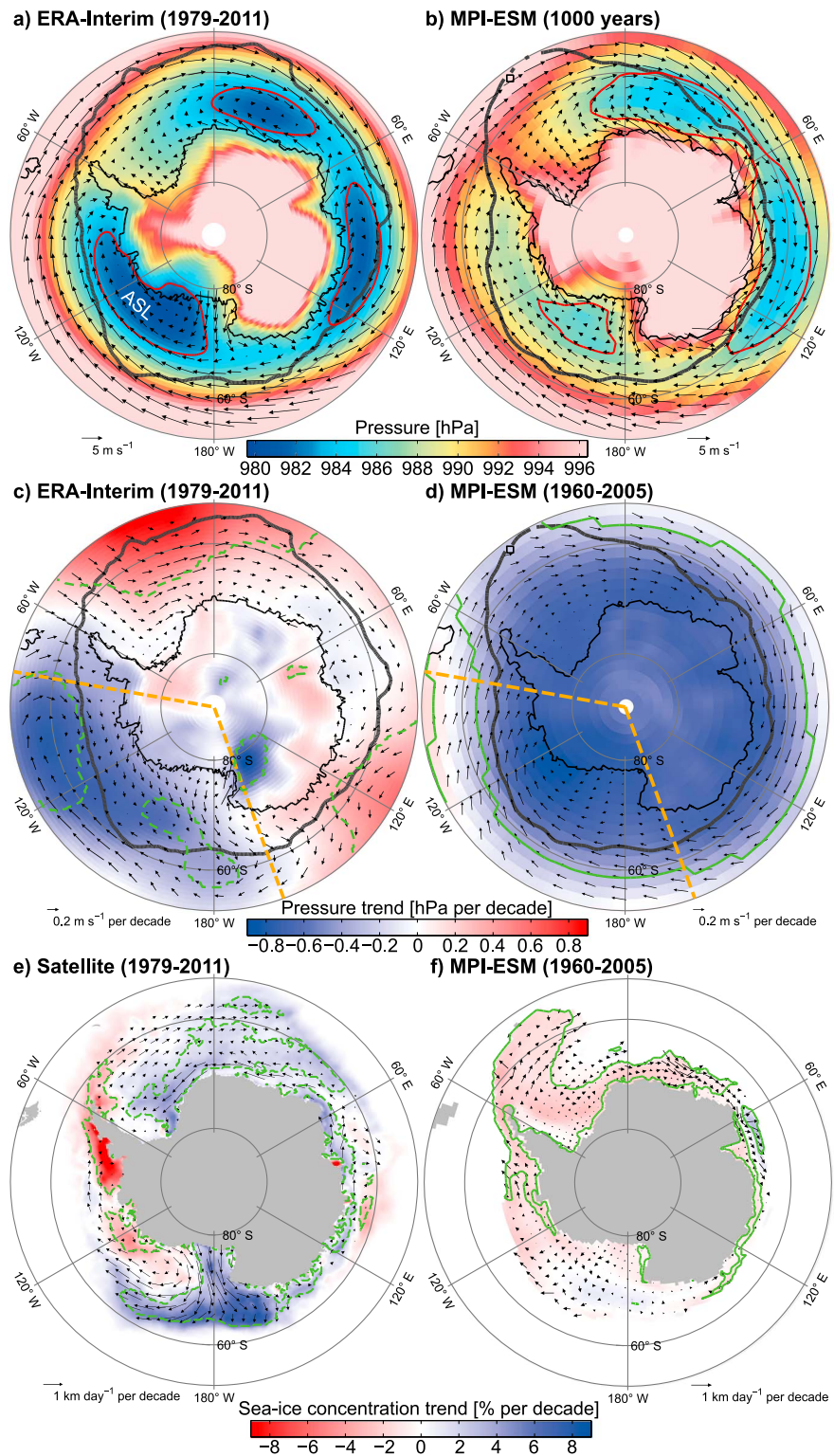
Figure 2. Annual surface circulation driving Antarctic sea ice changes. (a) ERA-Interim mean (1979–2011) SLP (shading; red: 983 hPa isobar) and 10 m wind field (vectors). ASL: Amundsen Sea Low. (b) Simulated (preindustrial) mean SLP (red: 987 hPa isobar) and surface wind field. (c) ERA-Interim decadal SLP and 10 m wind field trends (1979–2011). (d) Simulated decadal SLP and wind field trends (1960–2005, Experiment 1). Black bold lines (Figures 2a–2d): mean annual ice edge. Dashed orange lines (Figures 2c and 2d): sector for Figure 3. (e) Observed (1979–2011) and (f) simulated (1960–2005, Experiment 1) decadal sea ice concentration (shading) and drift trends (vectors). Dashed and solid green lines: significance of SLP and ice concentration trends (90% confidence level).
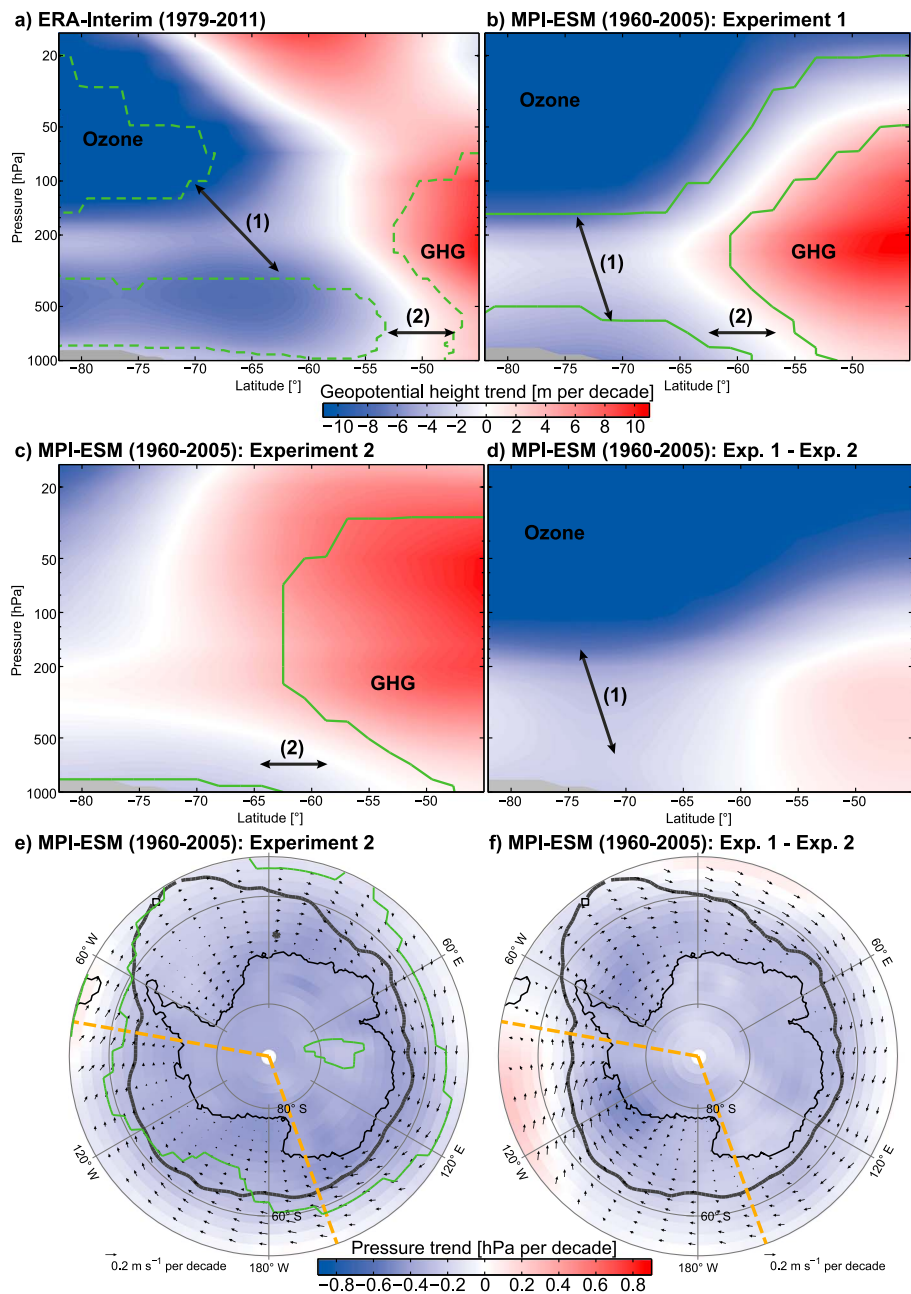
Figure 3. Attribution of annual surface circulation changes to (1) stratospheric ozone depletion and (2) GHG increase. Vertical cross sections of decadal zonal mean geopotential height changes between 160°E and 80°W (dashed orange lines in Figure 2). Experiments as in Figure 1. (a) ERA-Interim (1979–2011). (b) Simulations with all forcings (1960–2005). (c) Simulations without stratospheric ozone depletion illustrating mainly response to GHG increase (1960–2005). (d) Differences between simulations with (Figure 3b) and without stratospheric ozone depletion (Figure 3c) illustrating effect of ozone depletion. (e and f) As Figures 3c and 3d but for SLP (shading) and surface wind changes (vectors). Dashed orange lines: sector analyzed in Figures 3a–3d. Black bold lines: mean annual ice edge. Dashed and solid green lines: significance of geopotential height and SLP trends (90% confidence level).

They show that in global models, increased zonal winds enhance upwelling of warmer water from below that melts the ice. Figure 2d shows such a westward circulation intensification over most of the sea ice region, whereas in the ERA-Interim reanalysis intensified westerlies are mostly restricted to the Weddell Sea (Figure 2c). We conclude that the difference in the observed and simulated sea ice changes is caused by rather zonal simulated circulation changes and comparably small changes in the meridional winds in

the model simulations, which are caused by a weaker asymmetry in the SLP lowering. This also holds if the observational period 1979 to 2011 is analyzed in the model simulation (Figure S2).

The lowering of the high-latitude SLP leading to the zonal wind intensification in the model most likely results from anthropogenic forcing [*Thompson et al.*, 2011; *Lee and Feldstein*, 2013]. Consequently, we proceed to analyze whether the lowering of the SLP in the ASL region in the reanalysis, thus the sea ice changes, can also be attributed to these anthropogenic influences. We investigate annual mean geopotential height changes in vertical cross sections zonally averaged between 160°E and 80°W (dashed orange lines in Figures 2c and 2d). In the reanalysis data (1979–2011), we find three areas of significant (90% confidence level) geopotential height change (dashed green lines in Figure 2a). First, the cooling in regions of seasonal ozone depletion in the stratosphere leads to a lowering of the geopotential height there [*Thompson et al.*, 2011]. Second, the warming of the troposphere in lower latitudes, most likely caused by the GHG increase, increases the geopotential height there [*Santer et al.*, 2003]. As a consequence, the significant lowering of the geopotential height in the high-latitude troposphere is induced by a downward propagation of the stratospheric anomaly from ozone depletion (arrow 1, Figure 3a), by increasing GHGs and other changes in the external forcing (arrow 2), or by their combination [*Lee and Feldstein*, 2013].

Our simulations including both GHG increase and stratospheric ozone depletion (Experiment 1, Figure 3b) show a similar structure and magnitude of the geopotential height trends (1960–2005) as in ERA-Interim. However, discrepancies occur in the lower troposphere in high latitudes (south of 55°S), where modeled trends are slightly weaker, more confined to the surface, and occur at higher latitudes. The simulation with largely constant stratospheric ozone forcing (Experiment 2) results in a significant tropospheric geopotential height decrease in high latitudes (Figure 3c), but the trend is much weaker than in the simulation with all forcings (Figure 3b). The difference of the trends between the two experiments is primarily due to stratospheric ozone depletion (Figure 3d). Consequently, the SLP trends in the ASL region can mostly be explained by the combined effect of stratospheric ozone depletion and GHG increase (Figures 3e and 3f). If we analyze the model output only during the observational period (1979–2011; Figure S3), the effect of ozone depletion dominates the near-surface changes compared to the GHG increase, which is consistent with previous studies [*Thompson et al.*, 2011; *Lee and Feldstein*, 2013].

We conclude that the observed SLP lowering in the ASL region and the associated surface circulation changes (Figure 2c), thus the observed sea ice trends in this region, are influenced by the combination of anthropogenic ozone depletion and GHG increase, where the signal from ozone depletion presumably dominates. These conclusions are consistent with the suggestions by *Turner et al.* [2009]. We show that the difference in the sea ice response between global model simulations and observations occurs primarily due to the zonal distribution of the SLP response. A simulated rather zonal circulation intensification leads to a weak overall sea ice decline, consistent with *Bitz and Polvani* [2012], while the observed intensified meridional circulation induces strong regional changes and acts to increase the overall sea ice concentration in the period 1979 to 2011, consistent with *Holland and Kwok* [2012]. In the following, we will discuss whether this difference in the spatial distribution of the changes can be attributed to general shortcomings in the model circulation or to multidecadal natural variability.

4. Discussion

A rather zonally symmetric simulated SLP and circulation response to the anthropogenic forcing, as in our simulations, is a common feature among global models [*Son et al.*, 2010]. Yet this response is not consistent with, for example, observed asymmetric tropospheric geopotential height changes that have been related to stratospheric ozone depletion [*Neff et al.*, 2008]. The observed mean asymmetric circulation (Figure 2a) is related to orographic blocking effects [*Fogt et al.*, 2012], the asymmetric Antarctic land mass [*Lachlan-Cope et al.*, 2001], and topography-driven boundary layer wind systems [*Haumann*, 2011]. These arguments suggest that the too zonal near-surface circulation in the mean state and also the rather zonal response pattern over the sea ice in global models could be caused by a too smooth topography due to the models' coarse resolution and a not very realistic representation of the Antarctic surface climate. Our findings support this, since the response pattern differs mostly in the high-latitude troposphere in the ASL region (Figure 2) and the other sectors (40°W to 150°E; Figure S4).

The Antarctic sea ice response in global models to zonal wind changes as described by *Bitz and Polvani* [2012] and *Sigmond and Fyfe* [2014] is presumably sensitive to the vertical stability of the underlying ocean.

In MPI-ESM the high-latitude Southern Ocean vertical stability is underestimated [*Stössel et al.*, 2014], which is a common feature among global models [*Heuzé et al.*, 2013]. We hypothesize that a comparably unstable ocean responds with a stronger subsurface heat flux to increasing zonal winds, because the observed changes in the westerly wind component at the ice edge in the Weddell Sea (Figure 2c) lead to changes in the zonal advection of the ice (Figure 2e), whereas the westerly anomaly in the model (Figure 2d) leads to a decreasing ice cover (Figure 2f). Thus, the underlying mechanism responsible for the simulated sea ice changes seems to differ from the observed one. Even if the atmospheric circulation response was similar to the observed changes, the sea ice response could still differ from the observations, as it is the case in the Weddell Sea, for example.

Our result that the Antarctic sea ice response to the anthropogenic influence depends on the asymmetry of the SLP response is in line with the observed response of sea ice to interannual [*Fogt et al.*, 2012; *Simpkins et al.*, 2012] and multidecadal [*Li et al.*, 2014] variability. These studies show that sea ice changes strongly with the nonannular component of the SAM rather than with the zonally symmetric patterns, where a more positive SAM index is often associated with a lower SLP in the ASL region. However, the spatial structure of the sea ice changes associated with the positive SAM anomalies during the observational period differs from that of the observed trends [*Simpkins et al.*, 2012]. For example, while interannual variations mostly show a change of the strength of the ASL, in the observed trend the ASL additionally expands (see section 3). *Abram et al.* [2014] show that the SAM shifts to more positive values due to the anthropogenic forcing, which is consistent with both our model simulations and the pressure changes in the ERA-Interim reanalysis since the meridional pressure gradient increases (Figure 2). However, the effect that this has on the sea ice depends on the zonal structure.

Patterns of sea ice changes induced by multidecadal variability in the ASL SLP through connections with the tropics are similar to the observed trends [*Li et al.*, 2014]. Consequently, recent changes in the Antarctic sea ice might be influenced by natural variability. A multidecadal variability in the observed summertime air temperature records supports such an influence [*Fan et al.*, 2014]. Within the 1000 yearlong control simulation with MPI-ESM, about 9% of all possible 968 33 yearlong periods have an ASL SLP trend larger than the observed trend (averaged over the ocean surface south of 60°S and between 180°E and 80°W). This suggests that the currently observed Antarctic sea ice trends could also be fully explained by natural variability in the SLP and the related wind forcing. In turn, this would be inconsistent with a strong simulated circulation response to the anthropogenic influence. Thus, it is more likely that the observed changes are a mixture of an anthropogenic influence and multidecadal variations. Yet we cannot quantify their contributions since neither the pattern of the modeled sea ice variability nor that of the modeled response to the forcing currently reproduce the observed pattern of sea ice trends in coupled models.

Several other mechanisms have been suggested to contribute to the observed Antarctic sea ice changes. The recent freshening of the Southern Ocean could have increased the sea ice cover by stabilizing the water column [*Bintanja et al.*, 2013]. *Goosse and Zunz* [2014] suggested that the sea ice increase is largely driven by a positive ice-ocean feedback that decreases oceanic upwelling and might be initiated by changes in ice advection due to variations in the atmospheric circulation. However, as we show here, there is confidence that the dominant cause of observed sea ice changes are persisting changes in the atmospheric circulation because the patterns of circulation changes almost perfectly match those of ice drift and concentration in independent data sets over multidecadal time scales (cf. Figures 2c and 2e), confirming the findings by *Haumann* [2011] and *Holland and Kwok* [2012]. It is possible that these changes in atmospheric circulation cause additional feedbacks through changes in precipitation, oceanic upwelling, or gyre circulation. Atmospheric circulation changes, nevertheless, remain the most likely driver of the observed Antarctic sea ice changes independent of the question whether multidecadal variability or anthropogenic forcing is the underlying cause.

5. Summary and Conclusions

Combining observations with model simulations, we find that the recently observed Antarctic sea ice changes (1979–2011) are mostly driven by atmospheric circulation changes, which are in turn consistent with at least a partial anthropogenic influence. Satellite and reanalysis data show that intensified meridional winds increase the northward ice advection in the Ross Sea and meridional heat exchange in the Ross Sea and WAP regions, where the largest sea ice changes are observed. This confirms the findings by

Haumann [2011] and *Holland and Kwok* [2012] for the full observational period. These circulation changes are caused by a significant, zonally asymmetric lowering of the SLP, which is evident as an expansion and strengthening of the ASL.

Our model experiments (MPI-ESM) show that such SLP changes in this region can be explained by a combination of stratospheric ozone depletion and GHG increase (in line with *Son et al.* [2010]), where the former dominates during the observational period (1979–2011). We conclude that also the observed circulation-driven sea ice changes are influenced by these anthropogenic forcings (consistent with *Turner et al.* [2009]). However, similar to other global models [*Son et al.*, 2010], MPI-ESM's SLP response is rather zonally symmetric leading to a circumpolar westerly wind anomaly and little changes in meridional winds. A too zonally symmetric SLP compared to observations also occurs in the mean state and the natural variability. Thus, we argue that also the response to the anthropogenic influence might lack in zonal asymmetry, which might be caused by the coarse resolution of the Antarctic topography and inaccuracies of the representation of the Antarctic surface climate in the sea ice area in global models. Consistent with findings by *Bitz and Polvani* [2012] and *Sigmond and Fyfe* [2014], this zonal circulation change leads to a weak modeled overall sea ice decline, whereas regions that experience strengthened westerlies in the observations (e.g., the Weddell Sea) mostly show a zonal redistribution of the sea ice. We argue that an underestimated vertical stability of the underlying ocean in our model [*Stössel et al.*, 2014] and other global models [*Heuzé et al.*, 2013] might cause this difference. We conclude that most of the discrepancy between the observed and modeled Antarctic sea ice trends arises from the difference in the zonal distribution of SLP changes and the different sea ice response to zonal and meridional wind changes.

The model simulates multidecadal variations of SLP in the ASL region of comparable magnitude to the observed trends. This supports recent suggestions of an influence of multidecadal variability on observed sea ice trends [*Fan et al.*, 2014; *Li et al.*, 2014]. However, we show that the recent argument that observed sea ice changes could be purely driven by multidecadal variability [*Polvani and Smith*, 2013] is inconsistent with the simulated SLP response to the anthropogenic influence. A clear distinction between effects imposed by natural variability and anthropogenic forcing will only become possible once models accurately represent asymmetries in the near-surface circulation and the associated sea ice patterns.

References

Abram, N. J., R. Mulvaney, F. Vimeux, S. J. Phipps, J. Turner, and M. H. England (2014), Evolution of the Southern Annular Mode during the past millennium, *Nat. Clim. Change*, 4, 564–569, doi:10.1038/nclimate2235.

Bintanja, R., G. J. van Oldenborgh, S. S. Drijfhout, B. Wouters, and C. A. Katsman (2013), Important role for ocean warming and increased ice-shelf melt in Antarctic sea-ice expansion, *Nat. Geosci.*, 6(5), 376–379, doi:10.1038/ngeo1767.

Bitz, C. M., and L. M. Polvani (2012), Antarctic climate response to stratospheric ozone depletion in a fine resolution ocean climate model, *Geophys. Res. Lett.*, 39, L20705, doi:10.1029/2012GL053393.

Bracegirdle, T. J., and G. J. Marshall (2012), The reliability of Antarctic tropospheric pressure and temperature in the latest global reanalyses, *J. Clim.*, 25(20), 7138–7146, doi:10.1175/JCLI-D-11-00685.1.

Bromwich, D. H., J. P. Nicolas, and A. J. Monaghan (2011), An assessment of precipitation changes over Antarctica and the Southern Ocean since 1989 in contemporary global reanalyses, *J. Clim.*, 24(16), 4189–4209, doi:10.1175/2011JCLI4074.1.

Cionni, I., et al. (2011), Ozone database in support of CMIP5 simulations: Results and corresponding radiative forcing, *Atmos. Chem. Phys.*, 11(21), 11,267–11,292, doi:10.5194/acp-11-11267-2011.

Comiso, J. C., and F. Nishio (2008), Trends in the sea ice cover using enhanced and compatible AMSR-E, SSM/I, and SMMR data, *J. Geophys. Res.*, 113, C02S07, doi:10.1029/2007JC004257.

Dee, D. P., et al. (2011), The ERA-Interim reanalysis: Configuration and performance of the data assimilation system, *Q. J. R. Meteorol. Soc.*, 137(656), 553–597, doi:10.1002/qj.828.

Ding, Q., E. J. Steig, D. S. Battisti, and M. Kuttel (2011), Winter warming in West Antarctica caused by central tropical Pacific warming, *Nat. Geosci.*, 4(6), 398–403, doi:10.1038/ngeo1129.

Fan, T., C. Deser, and D. P. Schneider (2014), Recent Antarctic sea ice trends in the context of Southern Ocean surface climate variations since 1950, *Geophys. Res. Lett.*, 41, 2419–2426, doi:10.1002/2014GL059239.

Fogt, R. L., J. M. Jones, and J. Renwick (2012), Seasonal zonal asymmetries in the southern annular mode and their impact on regional temperature anomalies, *J. Clim.*, 25(18), 6253–6270, doi:10.1175/JCLI-D-11-00474.1.

Fowler, C., W. Emery, and M. Tschudi (2013), *Polar Pathfinder Daily 25 km EASE-Grid Sea Ice Motion Vectors, Version 2, 1979-2011*, Natl. Snow and Ice Data Cent., Boulder, Colo.

Giorgetta, M. A., et al. (2012a), CMIP5 simulations of the Max Planck Institute for Meteorology (MPI-M) based on the MPI-ESM-LR model: The historical experiment, served by ESGF, World Data Cent. for Clim.

Giorgetta, M. A., et al. (2012b), CMIP5 simulations of the Max Planck Institute for Meteorology (MPI-M) based on the MPI-ESM-LR model: The piControl experiment, served by ESGF, World Data Cent. for Clim.

Giorgetta, M. A., et al. (2013), Climate and carbon cycle changes from 1850 to 2100 in MPI-ESM simulations for the Coupled Model Intercomparison Project phase 5, *J. Adv. Model. Earth Syst.*, 5(3), 572–597, doi:10.1002/jame.20038.

Goosse, H., and V. Zunz (2014), Decadal trends in the Antarctic sea ice extent ultimately controlled by ice-ocean feedback, *The Cryosphere*, 8(2), 453–470, doi:10.5194/tc-8-453-2014.

Haumann, F. A. (2011), Dynamical interaction between atmosphere and sea ice in Antarctica, MSc thesis, Utrecht Univ., Utrecht, Netherlands.

Heuzé, C., K. J. Heywood, D. P. Stevens, and J. K. Ridley (2013), Southern Ocean bottom water characteristics in CMIP5 models, *Geophys. Res. Lett.*, *40*, 1409–1414, doi:10.1002/grl.50287.

Holland, P. R. (2014), The seasonality of Antarctic sea ice trends, *Geophys. Res. Lett.*, *41*, 4230–4237, doi:10.1002/2014GL060172.

Holland, P. R., and R. Kwok (2012), Wind-driven trends in Antarctic sea-ice drift, *Nat. Geosci.*, *5*, 872–875, doi:10.1038/ngeo1627.

Hosking, J. S., A. Orr, G. J. Marshall, J. Turner, and T. Phillips (2013), The influence of the Amundsen-Bellingshausen seas low on the climate of West Antarctica and its representation in coupled climate model simulations, *J. Clim.*, *26*(17), 6633–6648, doi:10.1175/JCLI-D-12-00813.1.

Jungclaus, J. H., N. Fischer, H. Haak, K. Lohmann, J. Marotzke, D. Matei, U. Mikolajewicz, D. Notz, and J. S. von Storch (2013), Characteristics of the ocean simulations in the Max Planck Institute Ocean Model (MPIOM) the ocean component of the MPI-Earth system model, *J. Adv. Model. Earth Syst.*, *5*(2), 422–446, doi:10.1002/jame.20023.

Kottmeier, C., J. Olf, W. Frieden, and R. Roth (1992), Wind forcing and ice motion in the Weddell Sea region, *J. Geophys. Res.*, *97*(D18), 20,373–20,383, doi:10.1029/92JD02171.

Lachlan-Cope, T. A., W. M. Connolley, and J. Turner (2001), The role of the non-axisymmetric Antarctic orography in forcing the observed pattern of variability of the Antarctic climate, *Geophys. Res. Lett.*, *28*(21), 4111–4114, doi:10.1029/2001GL013465.

Lee, S., and S. B. Feldstein (2013), Detecting ozone- and greenhouse gas–driven wind trends with observational data, *Science*, *339*(6119), 563–567, doi:10.1126/science.1225154.

Li, X., D. M. Holland, E. P. Gerber, and C. Yoo (2014), Impacts of the north and tropical Atlantic Ocean on the Antarctic Peninsula and sea ice, *Nature*, *505*(7484), 538–542, doi:10.1038/nature12945.

Mahlstein, I., P. R. Gent, and S. Solomon (2013), Historical Antarctic mean sea ice area, sea ice trends, and winds in CMIP5 simulations, *J. Geophys. Res. Atmos.*, *118*, 5105–5110, doi:10.1002/jgrd.50443.

Meier, W., F. Fetterer, M. Savoie, S. Mallory, R. Duerr, and J. Stroeve (2013), *NOAA/NSIDC Climate Data Record of Passive Microwave Sea Ice Concentration, Version 2, 1979-2011*, Natl. Snow and Ice Data Cent., Boulder, Colo., doi:10.7265/N55M63M1.

Neff, W., J. Perlwitz, and M. Hoerling (2008), Observational evidence for asymmetric changes in tropospheric heights over antarctica on decadal time scales, *Geophys. Res. Lett.*, *35*, L18703, doi:10.1029/2008GL035074.

Notz, D., F. A. Haumann, H. Haak, J. H. Jungclaus, and J. Marotzke (2013), Arctic sea-ice evolution as modeled by Max Planck Institute for Meteorology's Earth system model, *J. Adv. Model. Earth Syst.*, *5*(2), 173–194, doi:10.1002/jame.20016.

Olason, E., and D. Notz (2014), Drivers of variability in Arctic sea-ice drift speed, *J. Geophys. Res. Oceans*, *119*, 5755–5775, doi:10.1002/2014JC009897.

Polvani, L. M., and K. L. Smith (2013), Can natural variability explain observed Antarctic sea ice trends? New modeling evidence from CMIP5, *Geophys. Res. Lett.*, *40*, 3195–3199, doi:10.1002/grl.50578.

Santer, B. D., et al. (2003), Contributions of anthropogenic and natural forcing to recent tropopause height changes, *Science*, *301*(5632), 479–483, doi:10.1126/science.1084123.

Schmidt, H., et al. (2013), Response of the middle atmosphere to anthropogenic and natural forcings in the CMIP5 simulations with the Max Planck Institute Earth system model, *J. Adv. Model. Earth Syst.*, *5*(1), 98–116, doi:10.1002/jame.20014.

Schneider, D. P., C. Deser, and Y. Okumura (2012), An assessment and interpretation of the observed warming of West Antarctica in the austral spring, *Clim. Dyn.*, *38*(1-2), 323–347, doi:10.1007/s00382-010-0985-x.

Sigmond, M., and J. C. Fyfe (2014), The Antarctic sea ice response to the ozone hole in climate models, *J. Clim.*, *27*(3), 1336–1342, doi:10.1175/JCLI-D-13-00590.1.

Simpkins, G. R., L. M. Ciasto, D. W. J. Thompson, and M. H. England (2012), Seasonal relationships between large-scale climate variability and antarctic sea ice concentration, *J. Clim.*, *25*(16), 5451–5469, doi:10.1175/JCLI-D-11-00367.1.

Simpkins, G. R., S. McGregor, A. S. Taschetto, L. M. Ciasto, and M. H. England (2014), Tropical connections to climatic change in the extratropical southern hemisphere: The role of atlantic SST trends, *J. Clim.*, *27*(13), 4923–4936, doi:10.1175/JCLI-D-13-00615.1.

Son, S.-W., et al. (2010), Impact of stratospheric ozone on Southern Hemisphere circulation change: A multimodel assessment, *J. Geophys. Res.*, *115*, D00M07, doi:10.1029/2010JD014271.

Stammerjohn, S., D. Martinson, R. Smith, X. Yuan, and D. Rind (2008), Trends in Antarctic annual sea ice retreat and advance and their relation to El Nino-Southern Oscillation and Southern Annular Mode variability, *J. Geophys. Res.*, *113*, C03S90, doi:10.1029/2007JC004269.

Stevens, B., et al. (2013), Atmospheric component of the MPI-M Earth System Model: ECHAM6, *J. Adv. Model. Earth Syst.*, *5*(2), 146–172, doi:10.1002/jame.20015.

Stössel, A., et al. (2014), Controlling high-latitude southern ocean convection in climate models, *Ocean Modelling*, in press.

Thompson, D. W. J., S. Solomon, P. J. Kushner, M. H. England, K. M. Grise, and D. J. Karoly (2011), Signatures of the antarctic ozone hole in Southern Hemisphere surface climate change, *Nat. Geosci.*, *4*(11), 741–749, doi:10.1038/ngeo1296.

Turner, J., J. C. Comiso, G. J. Marshall, T. A. Lachlan-Cope, T. Bracegirdle, T. Maksym, M. P. Meredith, Z. Wang, and A. Orr (2009), Non-annular atmospheric circulation change induced by stratospheric ozone depletion and its role in the recent increase of Antarctic sea ice extent, *Geophys. Res. Lett.*, *36*, L08502, doi:10.1029/2009GL037524.

Turner, J., T. J. Bracegirdle, T. Phillips, G. J. Marshall, and J. S. Hosking (2013), An initial assessment of antarctic sea ice extent in the CMIP5 models, *J. Clim.*, *26*(5), 1473–1484, doi:10.1175/JCLI-D-12-00068.1.

Zunz, V., H. Goosse, and F. Massonnet (2013), How does internal variability influence the ability of CMIP5 models to reproduce the recent trend in Southern Ocean sea ice extent?, *The Cryosphere*, *7*(2), 451–468, doi:10.5194/tc-7-451-2013.